JOURNAL OF MATERIALS SCIENCE 29 (1994) 3080–3084

The failure of composite tubes due to combined compression and torsion

P. M. JELF, N. A. FLECK
Cambridge University Engineering Department, Trumpington Street, Cambridge CB2 1PZ, UK

The strength of unidirectional carbon-fibre epoxy laminates has been measured for combined compression and shear loading. Failure was by plastic microbuckling. The axial compressive strength decreased linearly to zero as the shear stress parallel to the fibres was increased from zero to the shear strength. These experimental results support the predictions of Budiansky and Fleck and suggest an average fibre misalignment angle of 2°–3°.

1. Introduction

A dominant failure mechanism of long-fibre polymeric matrix composites is microbuckling [1–10]. Microbuckling is a plastic shear instability, and occurs by the rotation of initially misaligned fibres within a well-defined band. Recent work by Budiansky and Fleck [5, 6] has shown theoretically that remote shear stresses activate yield within the microbuckle band and greatly reduce the compressive strength of the unidirectional composite. The purpose of the present study was to validate these predictions by measuring the compressive strength of pultruded carbon fibre–epoxy tubes under combined compression and torsion.

2. Theory

Unidirectional fibre composites fail in compression by a number of mechanisms [9, 11], including (i) matrix failure, (ii) fibre crushing, (iii) splitting from one end of the specimen, (iv) surface delamination driven by elastic buckling of a surface-debonded layer, (v) elastic microbuckling, and (vi) plastic microbuckling. Plastic microbuckling appears to be the dominant compressive failure mechanism for undamaged carbon fibre–epoxy composites.

Argon [1] and Budiansky [10] argue that plastic microbuckling is controlled by the shear yield strength, τ_y, of the matrix and the initial misalignment angle, $\bar{\phi}$, of the fibres, as defined in Fig. 1. It is assumed that the composite has a rigid–perfectly plastic shear response, and the fibres are taken to be inextensional. They show that the compressive strength, σ_c, for microbuckling in a band oriented transverse to the fibre direction (band orientation $\beta = 0$ in Fig. 1) is

$$\sigma_c = \frac{\tau_y}{\bar{\phi}} \tag{1}$$

More recent calculations by Fleck *et al.* [12] show that the bending stiffness of the fibre is sufficiently small to provide negligible enhancement to the compressive strength. Thus, a kinking analysis suffices for most practical cases, and we may ignore the role of fibre bending.

Microbuckle bands are typically oriented at a finite angle, β, in the range 10°–30°, where β is shown in Fig. 1. When β is finite, rotation of fibres within the microbuckle band involves both shear and transverse straining. In order to predict the compressive strength for finite β, a multi-axial yield surface is needed. Budiansky [10] assumed that the composite is endowed with a quadratic yield surface, of transverse yield stress, σ_{Ty}, and shear yield stress, τ_y.

The compressive strength of the composite is [10]

$$\sigma_c = \frac{\tau_y^*}{\bar{\phi}} \tag{2}$$

where $\tau_y^* \equiv \tau_y[1 + (\sigma_{Ty}/\tau_y)^2 \tan^2\beta]^{1/2}$. Typically, $\sigma_{Ty}/\tau_y \approx 2$, $\beta \approx 20°$ and τ_y^* is slightly greater than τ_y (i.e. $\tau_y^* \approx 1.2\tau_y$).

Fleck and Budiansky [5] have considered the microbuckling response of a rigid–perfectly plastic fibre composite subjected to both a remote compressive stress, σ^∞, and a remote shear stress, τ^∞. The critical compressive stress is found to be

$$\sigma_c = \frac{\tau_y^* - \tau^\infty}{\bar{\phi}} \tag{3}$$

which suggests that the compressive strength is severely knocked down by the presence of remote shear.

Considerable strain hardening is exhibited by polymer matrix composites: in order to make use of the rigid–perfectly plastic assumption an arbitrary definition for τ_y is required. Budiansky and Fleck [6] have recently included strain hardening in their kinking analysis by adopting the Ramberg–Osgood relation in shear

$$\frac{\gamma}{\gamma_y} = \frac{\tau}{\tau_y} + \frac{3}{7}\left(\frac{\tau}{\tau_y}\right)^n \tag{4}$$

The first term on the right-hand side of Equation 4 represents the elastic contribution, and the second term represents the plastic contribution to the total

0022–2461

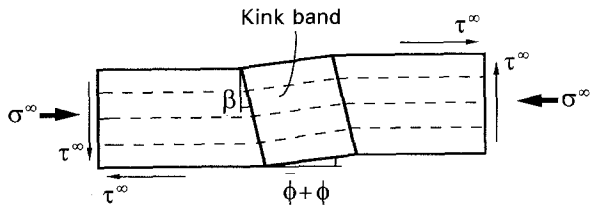

Figure 1 Idealized plastic microbuckle. The kink band is orientated at an angle β. It is assumed that fibres in the kink band have an initial (uniform) misalignment, $\bar{\phi}$, and rotate an additional angle, ϕ, under the remote loading.

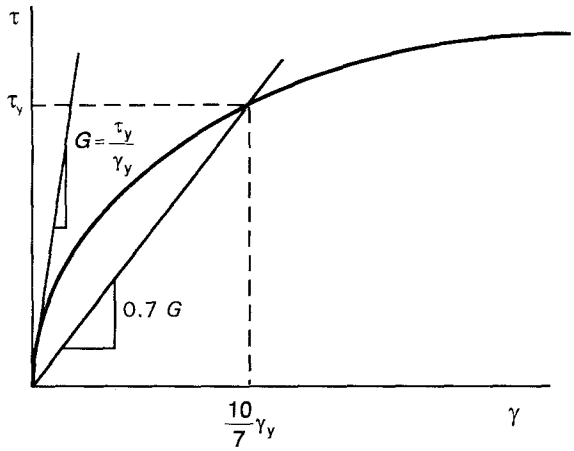

Figure 2 Deduction of Ramberg–Osgood parameters τ_y, γ_y and n from an experimental shear stress, τ, versus shear strain, γ, response for a unidirectional composite.

shear strain, γ. The parameters τ_y, γ_y and n are deduced from an experimental τ versus γ curve for the composite in the manner depicted in Fig. 2. The initial slope of the τ–γ curve defines the elastic shear modulus $G \equiv \tau_y/\gamma_y$. A line of slope $0.7G$ and passing through the origin intersects the line τ versus γ curve at $\gamma = 10\gamma_y/7$, $\tau = \tau_y$; this procedure fixes γ_y and τ_y. Finally, the index n is deduced by fitting Equation 4 to the τ versus γ curve at $\gamma = 5\gamma_y$; this procedure gives almost the same value for n as a least squares curve fit.

The kinking analysis of Budiansky and Fleck [6] suggests that the uniaxial compressive failure strength, σ_c, of a unidirectional composite in the absence of remote shear is,

$$\sigma_c = G\left[1+\left(\frac{\sigma_{Ty}}{\tau_y}\right)^2\tan^2\beta\right]\Big/1+n\left(\frac{3}{7}\right)^{1/n}\left[\frac{\bar{\phi}}{(n-1)\gamma_y^*}\right]^{n-1/n} \quad (5a)$$

where

$$\gamma_y^* = \gamma_y\Big/\left[1+\left(\frac{\sigma_{Ty}}{\tau_y}\right)^2\tan^2\beta\right]^{1/2} \quad (5b)$$

In the limit of $\beta = 0°$ and a rigid–perfectly plastic shear response ($G\gamma_y \to \tau_y$, $\gamma_y \to 0$ and $n \to \infty$), Equation 5a and b reduce to Equation 1.

No simple analytical expression can be derived for the combined compression–shear strength of a fibre composite obeying the Ramberg–Osgood relation in pure shear. Budiansky and Fleck [6] have derived implicit equations for the axial strength of a composite subjected to a fixed remote shear stress, τ^∞. The axial stress, σ^∞, versus fibre rotation, ϕ, response is given by

$$\sigma^\infty - 2\tau^\infty\tan\beta = \frac{([1+(\sigma_{Ty}/\tau_y)^2\tan^2\beta]\phi+\gamma^\infty)\tau_e - \tau^\infty\gamma_e}{(\phi+\bar{\phi})\gamma_e} \quad (6)$$

where the effective strain in the kink band, γ_e is related to the fibre rotation, ϕ, in the band, and the remote shear strain, γ^∞, by

$$\gamma_e^2 = [1+(\sigma_{Ty}/\tau_y)^2\tan^2\beta]\phi^2+2\phi\gamma^\infty+(\gamma^\infty)^2 \quad (7)$$

The effective shear stress, τ_e, in the kink band is related to γ_e via the Ramberg–Osgood Equation 4, but with (τ, γ) replaced by (τ_e, γ_e). For a fixed value of τ^∞, the collapse response is obtained by calculating the remote stress, σ^∞, as a function of ϕ via Equations 4, 6 and 7; the compressive strength is given by the maximum value attained by σ^∞.

3. Compression–torsion tests

3.1. Specimen preparation

Compression–torsion tests were performed on pultruded carbon fibre–epoxy tubes (supplied by Fibreforce Composites Ltd, Fairoak Lane, Runcorn, Cheshire, UK), consisting of EXAS HSI carbon fibres in DX 6002 epoxy matrix. The fibres, of volume fraction 65%, were aligned parallel to the axis of the tube.

The tubes were of outside diameter 25.5 mm and wall thickness 3.4 mm; they were cut to a specimen length of 160 mm, and mounted on a tapered mandrel to allow the outside diameter to be ground concentrically to the bore. Specimens were ground to the waisted profile shown in Fig. 3, in order to ensure failure within the guage section. Finally, each specimen was mounted on a lathe and the ends turned down to ensure that the end faces were perpendicular to the specimen axis.

3.2. Test method

Tests were performed on a tension–torsion servo-hydraulic machine. The specimen was gripped by split collar grips, and a mandrel was inserted into the bore of each specimen during testing to minimize bending. (The mandrel was split at mid-length and the two halves were held 5 mm apart in the centre of the gauge

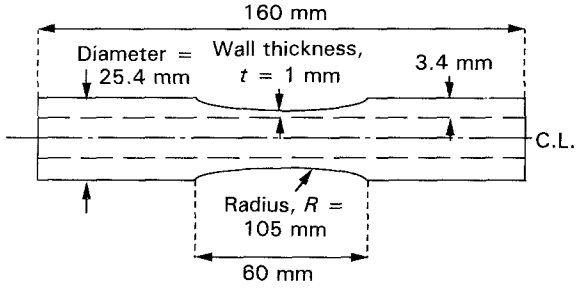

Figure 3 Compression–torsion specimen geometry.

section by a foam insert. Thus the specimen was unsupported over a length of 5 mm, which is sufficiently short to obviate macro-buckling.)

In order to monitor bending of the specimen associated with grip misalignment, four axial strain gauges were glued to each specimen. The gauges were equally spaced around the circumference of specimen and were placed at mid-length. The degree of bending was measured using small axial and torsional pre-loading, and was reduced to a negligible level by placing thin shims between the mating faces of the lower grip flange and the test machine.

Compression tests were performed on the tubes at a constant displacement rate of 0.017 mm s^{-1}; torsion tests were performed at an angular displacement rate of 1.7×10^{-3} rad s^{-1}. Combined compression–torsion tests were performed by applying a fixed torque and then by increasing the axial displacement until the specimen failed. The specimens were sufficiently thin for an applied torque to give a uniform shear stress across the gauge section.

4. Results

Under pure torsion, the tubes failed at $\tau = 77$ MPa and $\gamma = 8.3\%$; the failure mechanism was splitting parallel to the fibre direction as shown in Fig. 4. Under pure compression, and combined compression–torsion, failure was by plastic microbuckling.

Three to six tests were performed for each prescribed value of shear stress, τ^∞, and the average compressive strengths, σ_c, are shown in Fig. 5 as a function of τ^∞. The compressive strength, σ_c, decreases linearly with increasing $|\tau^\infty|$, until failure occurs by shear when τ^∞ equals the shear strength of the composite. Microbuckling occurs in the compression–torsion tests by the development of a single microbuckled band on a helix around the waisted gauge section. The microbuckle was arrested after propagating around one circumference of the tube by the formation of an axial split between the start and end of the microbuckle. The helix angle, β, was found to be 10° to 15° for $\tau^\infty > 0$, and $-10°$ to $-15°$ for $\tau^\infty < 0$, as shown in Fig. 6.

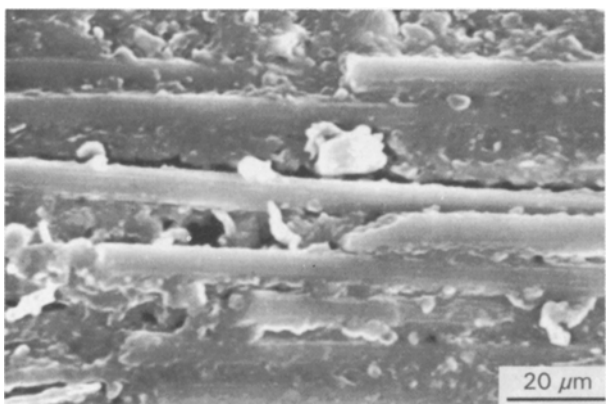

Figure 4 Electron micrograph of surface of tube tested in torsion alone, showing interfacial splitting behaviour. The fibres are aligned with the axis of the tube.

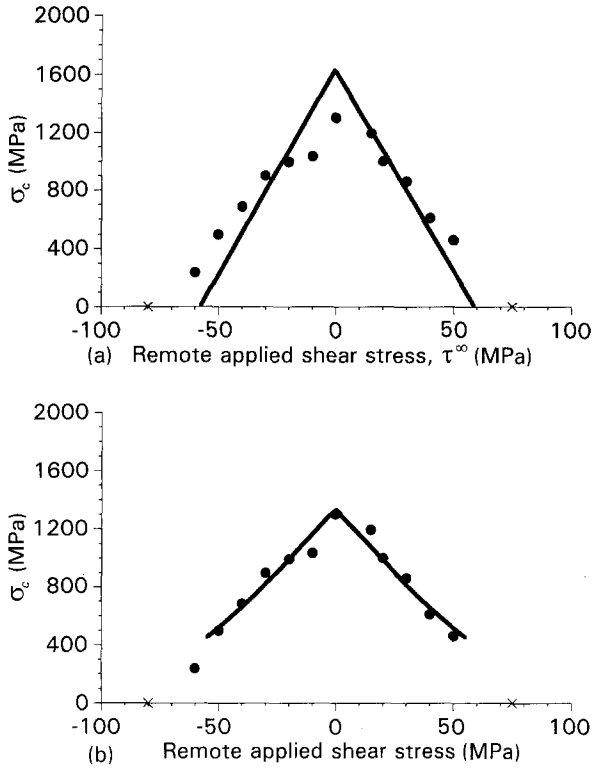

Figure 5 Variation of axial compressive strength of tubular specimens with applied remote shear stress. (a) The rigid–perfectly plastic theory is given by Equation 3; (———) theory, $\bar{\phi} = 2.0°$. (b) The strain-hardening theory is given by Equations 6 and 7; (———) theory, $\phi = 1.8°$. (×) Splitting failure, (●) kinking failure.

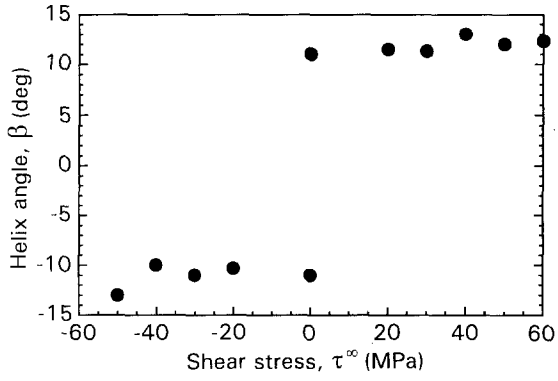

Figure 6 Effect of applied remote shear stress upon inclination, β, of kink band.

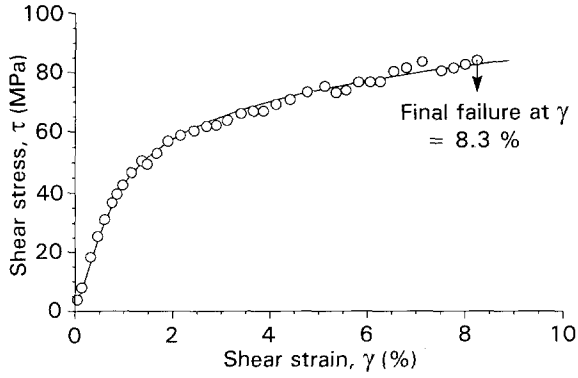

Figure 7 Comparison of (———) Ramberg–Osgood characterization ($\alpha = 3/7$, $n = 5.6$, $G = 5.12$ GPa, $\tau_y = 50.5$ MPa) experimental in-plane shear stress-strain data for the Carbon/Epoxy tube material.

The shear stress versus shear strain data necessary to determine the Ramberg–Osgood parameters for the carbon–epoxy material were obtained from a torsion test on the pultruded tubes. The shear strain was measured by strain gauges on the specimen, and the τ–γ response is given in Fig. 7.

5. Comparison of measured strength with predictions of the rigid–perfectly plastic theory

In order to compare the predictions of the microbuckling theory for a rigid–perfectly plastic solid with the measured compressive strengths, we need to define a representative shear yield stress, τ_y, from the τ–γ curve. We take arbitrarily τ_y to be that defined by the Ramberg–Osgood characterization; thus $\tau_y = 50.5$ MPa and $\beta = 15°$, and σ_{Ty}/τ_y is estimated to equal 2. Further, we assume $\bar{\phi} = 2.0°$ in order to produce the best fit to the experimental results (see Fig. 5a). This value for the waviness angle, $\bar{\phi}$, is in reasonable agreement with measured angles of $\bar{\phi}$ in fibre composites [9, 13]. A longitudinal section of the carbon fibre–epoxy material is shown in Fig. 8. It is clear from the micrograph that a value for $\bar{\phi}$ of 2° is reasonable.

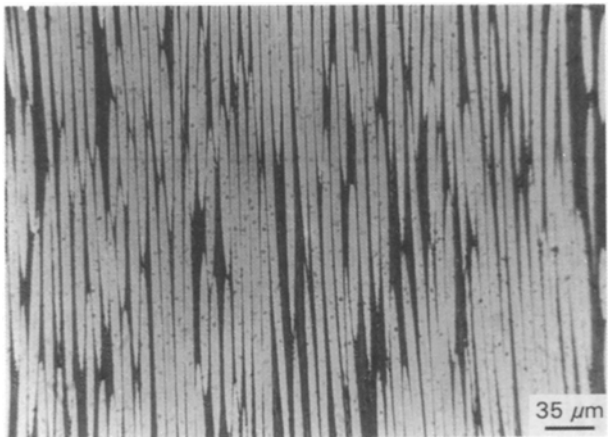

Figure 8 Polished section of carbon–epoxy tube, showing fibre arrangement.

5.1. Comparison of measured strength with predictions for strain-hardening material

The Ramberg–Osgood curve fit to the shear τ–γ is added to Fig. 7. A satisfactory fit is achieved by taking $\tau_y = 50.5$ MPa, $\gamma_y = 0.99\%$ ($G \equiv \tau_y/\gamma_y = 5.12$ GPa) and $n = 5.6$. These values are substituted into Equations 6 and 7 and the resulting predictions of the microbuckling theory are compared with the measured compression–torsion data in Fig. 5b. Good agreement is achieved by assuming $\bar{\phi} = 1.8°$. This inferred value for $\bar{\phi}$ is comparable to that for the rigid–perfectly plastic composite ($\bar{\phi} = 2.0°$).

6. Prediction of compressive strength for other composites

Table I gives the Ramberg–Osgood parameters for the shear response of several composite systems, together with compressive strength data in the absence of remote shear. The data have been either measured in the authors' laboratory or have been taken from the literature. Typically, the shear response is measured by performing tensile tests on $\pm 45°$ laminates; uniaxial compressive strengths were determined from modified Celanese tests. Equations 5a and b were used to infer a fibre misalignment angle, $\bar{\phi}$, for each composite, assuming $\beta = 20°$ and $\sigma_{Ty}/\tau_y = 2$ throughout. The misalignment angle, $\bar{\phi}$, is greatest for carbon–carbon composite ($\bar{\phi} = 3.1°$) and is least for carbon fibres in epoxy or in PEEK ($\bar{\phi} \approx 2.5°$). The fact that $\bar{\phi}$ decreases with increasing test temperature for AS4 carbon fibre–PEEK supports the notion that waviness is due to shrinkage during cool-down after consolidation.

7. Conclusions

Carbon fibre/epoxy tubes under combined axial compression and torsion fail by plastic microbuckling. Microbuckles form helically around the tube at an inclination $\beta = 10°$–$15°$ to the transverse direction.

TABLE I Ramberg–Osgood parameters and compressive failure strengths for various composite materials

Material	G (GPa)	τ_y (MPa)	γ_y (%)	γ_y^* (%)	n	σ_c (MPa)	$\bar{\phi}$ (deg)
AS4/PEEK	5.45	46.4	0.85	0.69	4.7	1109	2.79
Carbon fibre/epoxy tube material	5.12	50.5	0.99	0.80	5.6	1302	2.22
Part-cured T800/924c	5.67	41.9	0.74	0.60	10.3	734	3.70
T800/924c	6.78	62.5	0.92	0.75	3.5	1615	2.78
AS4/PEEK[a]							
$T = 23\,°C$	5.52	41.3	0.75	0.60	4.6	1109	2.49
$T = 77\,°C$	5.85	30.2	0.52	0.42	4.5	1070	2.02
$T = 132\,°C$	3.04	16.0	0.53	0.43	3.4	790	1.41
Carbon–carbon[b]	2.24	2.1	0.09	0.08	2.9	140	3.10

[a] The shear stress–strain data for AS4/PEEK at various temperatures are taken from [14]. The elevated temperature compression tests were performed by the authors.
[b] Data from [7].

The value for β is independent of the magnitude of the imposed shear stress, τ^{∞}.

We found that the axial compressive strength decreases in a linear manner with increasing applied shear stress. The rigid–perfectly plastic theory, Equation 3, fits the data well for an assumed fibre misalignment angle $\bar{\phi} = 2.0°$. A more sophisticated strain-hardening theory (Equations 6 and 7) is accurate for $\bar{\phi} = 1.8°$. Both values of $\bar{\phi}$ are within the range of independent measurements of $\bar{\phi}$, given, for example, by Yurgatis [13]. Finally, we list Ramberg–Osgood parameters for in-plane shear of a large number of unidirectional composites.

Acknowledgements

This work was carried out with the financial support of the Defence Research Agency of the Ministry of Defence, and the Science and Engineering Research Council (SERC). Financial contribution from the Office of Naval Research (ONR) contract 00014-91-J-1916 is gratefully acknowledged. The authors are grateful for helpful discussions with Dr P. T. Curtis and Professor B. Budiansky.

References

1. A. S. ARGON, "Fracture of Composites", Treatise of Material Science and Technology, Vol. 1 (Academic Press, New York, 1972).
2. C. R. CHAPLIN, *J. Mater. Sci.* **12** (1977) 347.
3. A. G. EVANS and W. F. ADLER, *Acta Metall.* **26** (1978) 725.
4. E. G. GUYNN and W. L. BRADLEY, *J. Compos. Mater.* **23** (1989) 479.
5. N. A. FLECK and B. BUDIANSKY, in "Inelastic Deformation of Composite Materials", edited by G. J. Dvorak (Springer, New York, 1990) pp. 235–74.
6. B. BUDIANSKY and N. A. FLECK, *J. Mech. Phys. Solids* **41**(1) (1993) 183.
7. S. B. BATDORF and R. W. C. KO, "Stress–strain Behaviour and Failure of Uniaxial Composites in Combined Shear and Compression, Parts I and II", Internal Report, School of Engineering and Applied Science, University of California, Los Angeles, CA 90024 (1987).
8. C. SOUTIS and N. A. FLECK, *J. Compos. Mater.* **24** (1990) 536.
9. P. M. JELF and N. A. FLECK, *ibid., J. Compos. Mater.* **26** (1992) 2706.
10. B. BUDIANSKY, *Computers Struct.* **16**(1–4) (1983) 3.
11. J. W. HUTCHINSON and Z. SUO, in "Advances in Applied Mechanics", Vol. 28, edited by J. W. Hutchinson and T. Y. Wu (Academic Press, New York, 1991).
12. N. A. FLECK, L. DENG and B. BUDIANSKY, *J. Appl. Mech.*, submitted.
13. S.W. YURGATIS, *Compos. Sci. Technol.* **30** (1987) 279.
14. E. G. GUYNN, W. L. BRADLEY, O. O. OCHOA and J. D. WHITCOMB, "A Comparison of Experimental Observations and Numerical Predictions for the Initiation of Fiber Microbuckling in Notched Composite Laminates", presented at 3rd ASTM Symposium on Composite Materials, Lake Buena Vista, Florida, 6–9 November 1989.

Received 17 August 1992
and accepted 24 August 1993